Clim. Past Discuss., 5, 1697–1729, 2009
www.clim-past-discuss.net/5/1697/2009/

Climate of the Past Discussions

Climate of the Past Discussions is the access reviewed discussion forum of *Climate of the Past*

An introduction to stable water isotopes in climate models: benefits of forward proxy modelling for paleoclimatology

C. Sturm[1], **Q. Zhang**[1], **and D. Noone**[2]

[1]Bert Bolin Centre for Climate Research, Stockholm University, Stockholm, Sweden
[2]ATOC & CIRES, University of Colorado, Colorado, USA

Received: 10 June 2009 – Accepted: 15 June 2009 – Published: 30 June 2009

Correspondence to: C. Sturm (christophe.sturm@geo.su.se)

Published by Copernicus Publications on behalf of the European Geosciences Union.

Abstract

Stable water isotopes have been measured in a wide range of climate archives, with the purpose of reconstructing regional climate variations. Yet the common assumption that the isotopic signal is a direct indicator of temperature proves to be misleading under certain circumstances, since its relationship with temperature also depends on e.g. atmospheric circulation and precipitation seasonality. The present article introduces the principles, benefits and caveats of using climate models with embedded water isotopes as a support for the interpretation of isotopic climate archives. A short overview of the limitations of empirical calibrations of isotopic proxy records is presented, with emphasis on the physical processes that infirm its underlying hypotheses. The simulation of climate and its associated isotopic signal, despite difficulties related to downscaling and intrinsic atmospheric variability, can provide a "transfer function" between the isotopic signal and the considered climate variable. The multi-proxy data can then be combined with model output to produce a physically consistent climate reconstruction and its confidence interval. A sensitivity study with the isotope-enabled global circulation model CAM3iso under idealised present-day, pre-industrial and mid-Holocene is presented to illustrate the impact of a changing climate on the isotope-temperature relationship.

1 Introduction

Climate change has become a major concern in recent years for scientists, policy makers and the general public alike (Solomon et al., 2007). This awareness brings into light two fundamental aspects for climatology research. First, climate is recognised as a variable in time; climate has changed in the past, in response to external (e.g. orbital, volcanic) forcing, and is likely to change in future due to human activities. Second, climate change is not defined by temperature change alone: rather than referring to "global warming", the attention is now focused on regional climate change patterns

CPD

5, 1697–1729, 2009

that include precipitation and atmospheric circulation variability. Hence there is a need to understand the mechanisms driving the climate variability. These considerations highlight the importance of paleo-climatology research. Reconstructing past climate variability and identifying its drivers improves our understanding of the complex Earth system dynamics, which lay the basis for reliable (hence operational) climate predictions.

Over the last decades, a major breakthrough in climatology research has been the use of climate models. Global circulation models (GCM) reproduce the dynamics of the atmosphere, later coupled to ocean dynamics (coupled or atmosphere-ocean GCM). The coupling allows to reproduce the interaction (or feedback) between both components of the Earth system, which can enhance (positive feedback) or reduce (negative feedback) the impact of external forcing (e.g. change in insolation). The major challenge with GCM studies lies in their validation: if one major climate process is identified in the model world, it needs to be demonstrated that it happens in the real world as well, i.e. that it is not an artifact caused by the necessarily imperfect model parametrisations. The validation is particularly challenging for past climate simulations, since there are no direct observations of climate variables (e.g. temperature, precipitation amounts, atmospheric pressure) prior to 1750. We can only rely on indirect indications (referred to as climate proxies), which require proper interpretation to reconstruct past climate change.

Stable water isotopologues ($H_2^{18}O$ and HDO), commonly referred to as stable water isotopes (SWI), are widely used as climate proxies. They can be seen as a "common currency" among many different types of climate archives. SWI have been measured in ice-cores, lake and marine sediments, speleothems, tree-ring and peat-bog cellulose etc. The recent inclusion of SWI fractionation parametrisations in climate models (Jouzel et al., 1987b; Hoffmann et al., 1998), an example for "forward proxy modelling", makes it possible to compare directly model output with the measured isotopic signal in climate archives, without requirement of a prior reconstruction of climate variables (known as "inverse proxy modelling").

CPD
5, 1697–1729, 2009

The present article aims to present the principles, benefits and caveats of applying GCM with SWI diagnostics in paleo-climatology. The first section introduces an historical overview of the "classical" interpretation of isotopic climate archives, raising some inherent limitations of the inverse proxy modelling approach. The second section presents the main principles for the implementation of SWI in climate models; rather than entering into technical details, it aims to present which scientific questions can and cannot be addressed with SWI-enabled GCM. The last section illustrates the issues raised in the previous sections: by comparing idealised simulations of present (1950), pre-industrial (1870) and mid-Holocene (6 ka BP) time-slices, we focus on the importance of atmospheric circulation and seasonality changes to explain the non-linearity between temperature and SWI composition in precipitation.

2 Empirical climate reconstruction from isotopic archives

2.1 Dansgaard temperature effect

Stable water isotopes have been measured in water bodies (rain, ocean surface, polar snow, lakes or rivers) from the early 1950's on. The isotopic composition is given as a deviation from the ocean reservoir with the delta notation, in permille: $\delta^{18}O=(R_{sample}/R_{SMOW}-1)\cdot 1000$, where $R=[H_2^{18}O]/[H_2^{16}O]$ is the concentration ratio between the heavier isotopologue and the common water molecule, SMOW stands for Standard Mean Ocean Water. The same notation is applied for water molecules including deuterium (HDO) to define δD. From 1961 onwards, the International Atomic Energy Agency (IAEA) and the World Meteorological Organisation (WMO) initiated the Global Network for Isotopes in Precipitation (GNIP) (Rapley and Grassl, 2009). A first synthesis and interpretation of the global isotopic measurements was presented by Dansgaard (1964).

In this founding article, Dansgaard states that "one cannot use the composition of the individual rain as a direct measure of the condensation temperature". Yet, "a simple

linear correlation between annual mean values of the surface temperature and the ^{18}O content in high-latitude, non-continental precipitation" can be obtained over Greenland, provided that "considerable accumulation occurs both in summer and winter", "the trajectories of precipitating air masses are roughly the same", "no considerable ablation takes places" and "topography of the considered area is simple". Under these conditions, the fractionation of heavy isotopes in precipitation corresponds to a Rayleigh distillation process (i.e. slow process with immediate removal of the condensate from the vapour after formation). Therefore, the $\delta^{18}O$ will show a significant correlation with the condensation temperature. Under the assumption that the vertical temperature profile in the atmosphere is roughly constant over the considered period, the mean annual condensation and surface temperatures will also be correlated, giving $\delta^{18}O = 0.67 \cdot T_{surf} - 13.6$.

The sum of conditions to be met when using the isotopic signal as a paleothermometer highlight the precautions needed before extending this method to isotopic archives other than Greenland ice-cores.

2.2 Application to isotopic archives

Following Dansgaard's initial work, the isotopic paleo-thermometer was used to reconstruct temperature changes over several glacial cycles from polar ice-cores. The recovery of long ice-cores from Antarctica (e.g. Vostok, Jouzel et al., 1987a, and Dome C, EPICA, 2004) as well as from Greenland (e.g. GRIP, Johnsen et al., 1995) revealed variations of $\delta^{18}O$ over several glacial cycles. Concomitant observations of temperature and $\delta^{18}O$ were requested in order to determine the $\delta^{18}O$-temperature relationship. Since no long-term observations of both $\delta^{18}O$ and temperature were available at these sites (for obvious logistical reasons), snow was sampled along traverses to determine the *spatial slope* of the $\delta^{18}O$-temperature regression, which was then used as an analogue for the *temporal slope* on which the paleo-thermometer relies. The validity of the method is discussed in Jouzel et al. (1997). Borehole thermometry represents an alter-

native method to reconstruct past temperature variations from the drilling site, independent of the δ^{18}O signal: knowing the (slow) diffusion of heat through the ice-sheet, the temperature profile along the drilling hole can be deconvoluted into variations of surface temperature. The estimates of temperature changes over Greenland between present-day and the Last Glacial Maximum (LGM) showed significant discrepancies between both methods: the δ^{18}O-T regression method implies only half of the temperature drop derived from borehole thermometry. These results were used by Johnsen et al. (2001) to determine a quadratic fit of δ^{18}O versus temperature, by combining borehole and δ^{18}O observations to obtain the best estimate of temperature changes over Greenland. A modelling study by Werner et al. (2000) provided a physical explanation for the discrepancy between both methods, related to a change in snowfall seasonality. According to a high-resolution simulation by ECHAM4 with embedded isotopes, most of the precipitation under LGM conditions occurred between May and September, while the precipitation peak at day occurs between September and November. Hence the present-day regression of mean annual δ^{18}O versus temperature was biased towards late autumn values, while the LGM δ^{18}O mainly records summer temperature. The borehole method on the other hand is not sensitive to the precipitation seasonality and therefore truly represents mean annual temperature estimates. The difference between the spatial and temporal slopes, and the role of seasonality, is illustrated in the third section of this article.

The interpretation of δ^{18}O as a climate proxy was also performed in non-polar environments. Ice-cores have been drilled in the (sub-)Tropics at high altitudes, e.g. in the Andean Cordillera in South America or summits in the Tibetan Himalayas (Thompson, 2000). On-site monitoring campaigns indicate that the isotopic signal under tropical conditions is not significantly correlated with temperature variations (Vimeux et al., 2005): water isotopes rather record the intensity of precipitation and can therefore be used to reconstruct past variability of the wet season. Furthermore, the interpretation of the isotopic signal is complicated to a larger extent than for polar environments by the impact of neighbouring vegetation, the origin of the moisture and convective pro-

cesses.

The analysis of δ^{18}O in ice-cores has long been a preferred climate archive, because the precipitation signal is recorded with only little post-deposition perturbation. Unfortunately, the geographical extent of ice-caps suitable for isotopic analysis is limited, while the regionalisation of (past and future) climate change has become a major challenge for the climate community. The analysis of the isotopic signal recorded in terrestrial archives can therefore fill the gap from low to high latitudes. These include e.g. lake-sediments (with δ^{18}O records from ostracode calcite, diatom silicate or algae cellulose), sphagnum in peat-bogs, tree-ring cellulose or speleothem calcite. All these archives have a particular record length and resolution, and take up ^{18}O from original precipitation in different ways, each affected by seasonality. Nevertheless, all terrestrial isotopic proxies are related to the hydrological cycle, and ^{18}O can therefore be regarded as a "common currency" to combine available proxy records into a comprehensive picture of climate change. The physical interpretation of the δ^{18}O signal in terrestrial archives is arduous, because on top of the processes governing the δ^{18}O variability in precipitation, local hydrological (runoff, infiltration) and biological processes need to be accounted for.

2.3 Inherent limitations of temperature-δ^{18}O regressions

As illustrated by the studies above, the reconstruction of temperature based on an isotopic archive is far from trivial. We can summarise the major issues raised in the discussions with following items.

(Non-)Stationarity of the T-δ^{18}O relationship

One major limitation with empirical climate reconstructions (or inverse proxy modelling) is the assumption that the isotopic signal is controlled by a single climate variable (e.g. temperature) in a uniform way throughout the entire proxy record. In other words, by applying the regression between δ^{18}O and e.g. temperature as obtained over the cal-

ibration period, one makes the implicit assumption that the relationship remains valid over the entire proxy record. In real cases, this stationarity assumption is rarely fulfilled, since climatic changes will often imply modifications of the atmospheric circulation patterns and changes in seasonality (see following items).

Impact of changing atmospheric circulation patterns

The isotopic composition of precipitation (and hence in the climate archive) is a result of fractionation processes along the air mass trajectory. This integrated signal is correlated with local parameters (e.g. local temperature) only as long as the trajectories are roughly similar throughout the study period. When studying large temperature shifts (e.g. over the Holocene), these are likely to imply severe modifications of the regional energy budget, which are likely to affect the regional circulation patterns.

Impact of changing seasonality

Most of the archives used for climate reconstruction are (at most) annually resolved. These annual records are seasonally biased: ice-cores record a climate signal only when precipitation occurs, tree-rings grow during summer using summer rain as well as melt water from winter snowfall. If the overall climate is changing, the seasonal distribution of precipitation is likely to be affected, as well as the timing and duration of the growing season.

In conclusion, the present section highlights some of the fundamental advances made in the interpretation of the isotopic signal in climate archives. As mentioned in the cited studies, the reconstructions are based on implicit assumptions which are impossible to verify under past climate conditions. The next section presents how climate models, fitted with stable water isotope diagnostics, can help assessing the temporal and spatial variability of isotopes in precipitation, to support paleo-climatological reconstructions.

3 Implementation of stable water isotopes in climate models

3.1 Fundamentals of climate modelling

Atmospheric global circulation models (A-GCM) are computer programmes which reproduce the state and dynamics of the atmosphere (and related components, e.g. land-surface) in a discrete way. In other words, the atmosphere is approximated by a collection of boxes, with horizontal extent typically in the order of one to five degrees (100–500 km) and 20–40 levels in height reaching the lower stratosphere. GCMs are similar to numerical weather forecast models, with the distinction of not being re-initialised with assimilated observations every 6 h.

The GCM code structure is divided into two components: the dynamical core and the physics parametrisations. The GCM dynamical core resolves the primitive equations governing the atmosphere thermo-dynamics (Bjerknes, 1921). These nonlinear differential equations express the conservation of momentum, energy and mass. The conservation of momentum is expressed by the Navier-Stockes equation, under the assumption of hydrostatic equilibrium (i.e. vertical acceleration is neglected). The conservation of energy is expressed as an energy budget, accounting for radiative processes through the atmosphere and on the Earth surface. The conservation of mass is expressed by the continuity equation, for all considered components of the atmosphere (air, water in vapour, liquid and ice phase). GCM use different discretisations (e.g. Arakawa grids, spherical harmonics, pressure or sigma vertical levels) and optimised mathematical algorithm to resolve the primitive equations. The internal time-step of GCM depends on the grid resolution and algorithm chosen, and is typically in the order of 30 min.

Many processes occurring in the atmosphere cannot be resolved explicitly in the dynamical core, because they happen at a much smaller scales: convective cloud systems for instance develop over an area of a few kilometers, which is two orders of magnitude less than the grid resolution. Convection needs thus to be parametrised, in order to represent the mean precipitation and energy release over the entire grid-cell.

The changes in prognostic hydrological variables (e.g. atmospheric liquid and vapour content, temperature) related to convection is fed back to the dynamical core, so that the next iteration is computed with updated variables. It is beyond the scope of the present article to describe details of GCM parametrisations. In the next sub-section, we will focus on parametrisations relevant for the inclusion of stable water isotope tracers.

3.2 Implementation of stable water isotope tracers in GCMs

The principles for implementing stable water isotope tracers in GCM are quite simple. The hydrological cycle needs to be duplicated, i.e. every variable in the source code related to water needs to be accompanied by its isotopic counterpart (for $H_2^{18}O$, HDO, and more recently $H_2^{17}O$). Hence, the dynamical core can advect and mix isotopic tracers from different air masses. In the physical parametrisations, every time a phase change of water takes places (for each internal time-step, i.e. roughly 30 min), the equilibrium and kinetic fractionation needs to be computed for all water phases (liquid water, vapour and ice), which allows a modification of the isotopic composition of different reservoirs across the globe. Knowing that a GCM source code consists of hundreds of subroutines making out tens of thousands of code lines, of which at least half are related to the hydrological cycle, the reader will realise what daunting task it represents to implement the isotopic tracers in the code, even though the underlying physics are relatively simple. It is beyond the scope of the present article to describe the technical aspects of the implementation. For further reading, an good description is given in Noone and Sturm (2009). Hereafter, we will summarise the major steps.

The implementation of isotopic tracers in the dynamical core focuses on the atmospheric prognostic variables (i.e. those needed to compute the state of the atmosphere in the next step). Depending on the GCM structure, the prognostic variables are water vapour, liquid water and/or ice. The inclusion of fractionation processes is treated in the physical parametrisations. Condensation into droplets or ice crystals is treated as an equilibrium fractionation under temperate conditions: the temperature-dependence of the fractionation coefficient was determined from lab experiments (Majoube, 1971).

At low temperature, a kinetic correction accounting for the slower diffusivity of heavier isotopes is applied (Jouzel and Merlivat, 1984). These fractionation processes are implemented in the cloud micro-physics, which is typically divided into large-scale (or stratiform) and convective precipitation. Once precipitation is formed in the cloud, up to 80% can re-evaporate in the under-saturated sub-cloud air. This implies a partial isotopic re-equilibration of the rain droplets with surrounding vapour: small, slowly falling droplets from large-scale precipitation re-equilibrate to 95%, while convective droplets re-equilibrate to 45%. This re-equilibration emphasises the importance of isotopic exchanges between the land-surface and precipitation: precipitation from small droplets will show an imprint of the local air moisture rather than the original cloud signature, which is important to bear in mind for subsequent proxy analysis. This however does not apply to snow, which makes polar archives easier to interpret as climate proxies.

Water fluxes over land play a major role in the isotopic hydrological cycle. The (isotopic) soil moisture keeps a memory of precipitation events (e.g. snow deposited in winter can melt and re-evaporate during summer), and is therefore a prognostic variable. Furthermore, plants evaporate through their leaves almost the entire water taken up by their roots; under steady-state conditions, transpiration is therefore non-fractionating (Bariac et al., 1994). Most GCM represent the soil moisture as a single reservoir (called "bucket" schemes), which does not allow the distinction between evaporation and transpiration. In this case, all evapo-transpiration is considered non-frationating. Recent efforts were made to implement isotopic tracers in multi-level soil moisture schemes, which allows the distinction. Such schemes are better appropriate to perform a comparison between terrestrial isotopic archives (e.g. tree-rings, speleothems) and model output. Finally, evaporation from the ocean surface is treated as equilibrium fractionation, with correction for the wind-dependent kinetic effects (Merlivat and Jouzel, 1979).

Following pioneering work in the 1980's by Joussaume et al. (1984); Jouzel et al. (1987b), water isotopes have been implemented in a growing number of GCM. It is worth noticing that most GCMs use very similar formulations for the isotopic fractionations, while the underlying physical parametrisations (e.g. for convection of land-surface

water fluxes) are far more diverse. A workshop (SWING2[1] – 2nd Stable Water Isotope iNtercomparison Group) was recently hosted by the Isotopic Hydrology Programme at the International Atomic Energy Agency (IAEA, Vienna) to perform an intercomparison of isotope-enabled GCM and their evaluation against observations of isotopes in precipitation from the Global Network for Isotopes in Precipitation (GNIP, Rapley and Grassl, 2009). All models participating in SWING2 are listed in Table 1. The simulations cover the last 50 years (or periods within), with 3 models (ECHAM4, GSM, LMDZ) being nudged to reanalyses (ERA40 or NCEP). In this case, the atmospheric circulation is forced to reproduce the observed weather while the (isotopic) water cycle is left unforced, which facilitates the direct comparison between observation and model output. In connection with the 3rd Paleoclimate Modelling Intercomparison Project (PMIP3), it is planned to organise a SWING3 experiment, where participating models will be compared under different climate conditions (e.g. last Millennium, Mid-Holocene, Last Glacial Maximum).

In addition to GCMs, stable water isotopes were recently implemented in regional climate models. The principles are identical, but simulating the climate over a smaller area enables to use a finer resolution (typically one order of magnitude, i.e. horizontal resolutions of 10–50 km). A isotope-enabled regional model requires to be nested in an isotopic GCM, to provide suitable lateral boundary conditions at a 6-h frequency. The jump in resolution imposes a shorter internal time-step, and therefore higher CPU demands; a reasonable simulation period is limited currently to a few decades. The 10 km limit in horizontal resolution is not simply determined by the computing capacities. Beyond this threshold, the hydrostatic assumption is no longer valid, nor e.g. the classical parametrisation for convection. To overcome this limitation, high resolution RCM have been developed recently, in which the water isotopes remain to be implemented. At present, two regional models with embedded isotopic module exist (Sturm et al., 2005; Yoshimura et al., personal communication, 2008).

[1]SWING2 simulations are available for download on the project's home-page http://people.su.se/~cstur/SWING2/.

3.3 What can and cannot be expected from isotopic paleo-simulations?

The preceding two subsections introduced the principles underlying the simulation of stable water isotopes within climate models. The present subsection aims to illustrate the benefits of such isotopic GCM for paleo-climatological studies. In particular, we focus on how simulations can complement the conventional interpretation of isotopic climate archives.

The major limitation of climate models consists in the fact that phenomena identified in the simulations have to be related to those happening in the real world. In the present article, we do not cover the inherent misfits in climate models. Despite the constant effort for improvement, the model parametrisations are still far from perfect, which has obvious consequences for the simulated $\delta^{18}O$ signal. Hence, every study involving climate simulations requires a thorough *validation* against observations for the study region. The validation of present-day simulations is often restricted by the scarcity and inherent measuring errors in observations; it becomes an even-more problematic task for simulations of past climates, where the interpretation of proxy records can partly rely on calibration from climate models. Besides the technical imperfections, mismatch between observed and simulated variables are related to (1) downscaling issues and (2) intrinsic variability of atmospheric processes.

As described earlier, a climate model reproduces the state of the Earth system on a discrete grid. Hence climate variables observed at a given site differ from the grid-cell mean over this location. The downscaling problem can be addressed with higher resolution climate models (e.g. regional circulation models). Yet, even when the horizontal resolution is 10 km instead of 100 km, the fundamental challenge of relating an area average to a point measurement remains. Statistical downscaling methods have been developed to match large-scale conditions with e.g. temperature and precipitation for a given location, taking into account local effects (e.g. lee- or wind-sided hill, small-scale impact of vegetation). Such statistical downscaling methods have not yet been extended to reproduce the isotopic content of precipitation.

CPD
5, 1697–1729, 2009

The intrinsic variability of climate constitutes an additional difficulty for the comparison between simulations and observations. Given a particular external forcing (e.g. orbital parameters for the insolation), the Earth system can adopt different, equally valid states. Yet the actual (observed) climate represents only one realisation of the many possible climate states. It is therefore not guaranteed that the climate model will reproduce the exact same solution as the one that actually occurred. This challenge has been tackled in different ways by the climate modelling community, which also holds for water isotope simulations. For present-day conditions, it is possible to constrain (or nudge) the atmospheric circulation in the model by assimilated observations (most commonly re-analyses, e.g. ERA40, ECMWF, 2003). Hence, the nudging technique ensures that a low-pressure system is reproduced roughly at the right place roughly at the right time, while the (isotopic) water cycle is left unconstrained. This enables a direct comparison between simulated and observed isotopic signal; as an example, three models in the SWING2 project (cf. Table 1) delivered nudged simulations over the 1958–2001 period. In study periods for which world-wide standard meteorological observations are lacking (typically prior to 1900), it is possible to conduct ensemble simulations. Taking identical external forcing, the simulations are launched with slightly different initial conditions, with the aim to cover several possible states of the climate system.

Given the above mentioned limitations, simulations of the δ^{18}O signal can be used in the following ways in complement to conventional isotopic proxy analyses. The advantages of having embedded water isotopes tracers (i.e. forward proxy modelling) is that the model output can be compared with the measured proxy (e.g. δ^{18}O in ice-cores). Hence, there is no need to derive a change in temperature and/or precipitation (with its associated inversion errors) from the proxy record before comparing it with the output of (non-isotopic) climate models. The isotope-enabled simulation can be seen as a platform, where all simulated variables are physically consistent with each other, and can be known at any location for any time. So even if, due to its intrinsic variability, the simulated δ^{18}O differs from the observed one, it is reasonable to as-

sume that the relationship between e.g. temperature and δ^{18}O in the model world will be equivalent to that of the real world. Hence, "transfer functions" between δ^{18}O and temperature can be derived from the simulation, to be later applied on the observed δ^{18}O signal in order to reconstruct actual temperature variations. Based on the internal coherence of the simulated climate, the "transfer function" approach can be extended to multi-proxy analysis. The multi-proxy records can both consist of similar climate archives at different locations (e.g. network of δ^{18}O in tree-ring cellulose over Europe) and/or different climate proxies at the same site (e.g. δ^{18}O and pollen distribution in the same peat-bog). This will give way to the *assimilation of proxy records* by forward proxy modelling. By incorporating several proxy records from different sites and origin, it is assumed that noise related to local processes will cancel out, to produce the best estimate changes in the study area. The a-priori knowledge of spatial patterns and seasonal variations, derived from climate simulations, is optimally combined with available proxy records to reconstruct a physically consistent picture of regional climate change. Furthermore, ensemble simulations deliver sufficient material for a thorough statistical analysis, which can add confidence intervals to the climate reconstruction.

4 Illustration: impact of radiation forcing on the simulated isotopic composition of precipitation

4.1 Experimental settings for the 3 simulations

The NCAR Community Atmosphere Model(CAM3.0) with embedded stable water isotopes (Noone et al., 2009) was used to perform three sensitivity experiments. The model is run on a 128×64 grid, i.e. with a horizontal resolution of 2.8×2.8°(roughly 300 km) and 19 vertical levels. The simulations reproduce idealised present day, pre-industrial and mid-Holocene climate conditions, respectively. Present day simulation is performed according to the AMIP1 protocol (Gates et al., 1999). Pre-industrial and mid-Holocene simulations follow the PMIP1 protocol (Joussaume and Taylor, 1995).

All the three simulations are forced by climatological sea-surface temperatures (SST) and sea-ice cover from the Hadley Ice and SST (HadiSST)/Reynolds dataset (Hack et al., 2002). The ice sheet topography and coastlines in all three simulations are set identical to present day.

The greenhouse gases and Earth's orbital parameters for the three simulations are listed in Table 2. In the current study, we consider the "pre-industrial" simulation to be the reference (control run). The "present" simulation has identical orbital forcing to the reference, but the atmospheric radiative budget is altered by higher concentrations of greenhouse gases (CO_2,CH_4 and NO_2) and aerosols. The main difference in insolation forcing for mid-Holocene, compared to pre-industrial, is related to the orbital parameters, which is represented by the eccentricity, obliquity and precession (Berger, 1978). The orbital parameters express the relative location of the Earth with respect to the sun, which affect the total amount and distribution of solar radiation across seasons: the Northern Hemisphere receives more solar radiation during (boreal) summer under mid-Holocene conditions, as illustrated in Fig. 1. The PMIP protocol also prescribes a change in atmospheric CH_4 concentrations, with a lower concentration at mid-Holocene.

For the sake of comparison, boundary conditions other than top-of-the-atmosphere insolation and greenhouse gas/aerosols were prescribed to be equal in all three simulations, according to the PMIP1 guidelines; in the real world, the sea-surface temperature, sea-ice cover and vegetation distribution were most likely different for the three periods, but incorporating these changes in the PMIP1 protocol would not allow to isolate the effect of radiation on climate. Present, pre-industrial and mid-Holocene should therefore not be understood as "best estimates" of the actual climate conditions, but rather as sensitivity experiments for the impact of the radiative budget on climate. Hence, the results shown hereafter represent a case study of changes of the radiative budget on atmospheric circulation, surface temperature and the $\delta^{18}O$ signal in precipitation.

4.2 Spatial patterns and seasonal variation in the reference run

The analysis of the reference run (pre-industrial radiation settings) introduces general features of GCM-simulated climate. The upper row in Fig. 2 shows the annual, winter and summer mean temperatures. As commonly expected, temperature undergoes a strong latitudinal control: it gets colder at higher latitudes. Furthermore, continentality imposes an additional control on temperature: at a given latitude, temperature tend to decrease when going away from the coast. This effect is not symmetrical: the temperature gradually decreases following the direction of the dominant winds. Therefore, the westerlies cause a west-east decreasing gradient over Eurasia, reaching lowest temperatures over Eastern Siberia, which is most noticeable in winter.

We aim to focus on the spatial patterns of the simulated δ^{18}O signal, as shown in the lower row of Fig. 2. At first order, δ^{18}O variations follow the temperature patterns: δ^{18}O decreases with higher latitudes, and reaches its minimum at the coldest places (Greenland, Eastern Siberia). A closer look reveals some differences. The *altitude effect* characterises the decrease in δ^{18}O with height. This is physically related to the Rayleigh distillation that takes place when an air parcel, lifted uphills, condenses to produce ever isotopically lighter precipitation. This explains the low δ^{18}O values over Greenland (−25 to −30‰ all year round). Furthermore, δ^{18}O experiences a stronger *continental effect* than temperature: at a given latitude, δ^{18}O decreases across Eurasia from −15‰ at Norway's Atlantic coast to −30‰ in Eastern Siberia in winter. The continental δ^{18}O effect is largely muted in summer, since the non-fractionating evapotranspiration recycles isotopically heavier moisture along the westerly trajectories.

In conclusion, the geographical patterns in temperature and δ^{18}O indicate that both are to a large extent controlled by atmospheric circulation patterns, which explains the fair agreement (rather than a strict physical control of local temperature on local δ^{18}O in precipitation). Furthermore, the annual mean in temperature and δ^{18}O result from a combination of seasonal processes, which are not necessarily related with each other. Therefore, deducing the processes of climate change from annually resolved archives

is not straightforward.

4.3 Response of temperature and δ^{18}O to changes in radiation settings

In order to identify the response of temperature and δ^{18}O patterns to a change in radiation settings (greenhouse gas and aerosols for the "present" experiment in Fig. 3, top-of-the-atmosphere radiation for the "mid-Holocene" experiment in Fig. 4), we will now consider the *difference* from the reference ("pre-industrial" experiment) for both temperature and δ^{18}O. First of all, it is worth noticing that the area-weighted annual mean in temperature over the domain is fairly small in these idealised simulations: the mean deviation for present is less than 0.01°C, while the mid-Holocene is +0.06°C warmer than the reference. The "present" simulation is colder in winter by −0.07°C, and almost equivalent in summer (−0.02°C). Due to the change in orbital forcing, the mid-Holocene simulation is colder than the reference in winter (−0.56°C), but significantly warmer in summer (+1.07°C), due to the stronger insolation (Fig. 1).

Despite the small changes in domain-wide means, both simulations exhibit distinct spatial patterns in their differences from the reference run, which vary according to the season. During winter (DJF), both simulations show a coherent pattern in temperature change: Alaska is up to 4°C warmer than the reference, while Eastern Siberia is up to 4°C colder (Figs. 3b and 4b). Similarly, Greenland's East coast warms up by up to 3°C, while its western coast experiences an equivalent cooling. These oscillation patterns are likely to be related to changes in the atmospheric circulation, such as the amplitude and location of stationary planetary waves in relation to the Arctic Oscillation.

Since the δ^{18}O signal is tributary to the stochastic behaviour of precipitation, the pattern of δ^{18}O changes is more patchy than that of temperature. Nevertheless some obvious features emerge, which infirm the strict interpretation of δ^{18}O as paleo-thermometer. First, the amplitude of δ^{18}O changes is not proportional to temperature changes. For instance, δ^{18}O in winter over Scandinavia and Western Russia experiences a large and wide-spread increase (Fig. 3f), which is far out of proportion with the change in temperature (Fig. 3c). Furthermore, the maximum in δ^{18}O change tends

to be located east of the maximum in temperature change (e.g. over Alaska), which implies that δ^{18}O has a stronger memory of processes occurring along its trajectory than temperature.

The interpretation of the δ^{18}O signal in summer is difficult, since it is influenced by local processes whose isotopic impacts are not strictly controlled by temperature (e.g. evapo-transpiration, convection). Since sea-surface temperatures and sea-ice cover are set equal for all 3 simulations, there are no noticeable changes in temperature over the Arctic Ocean. This does not prevent δ^{18}O from experiencing its strongest increases, as it is influenced by nearby terrestrial processes. Similarly, the overall summer warming over land in the "mid-Holocene" simulation (Fig. 4c), as a result of the stronger summer insolation (Fig. 1) does not translate into a uniform increase in δ^{18}O which inherits the δ^{18}O deficit from the melting lighter winter precipitation.

As a result from these seasonal variations, the annual mean changes for temperature and δ^{18}O no longer show consistent patterns between temperature and δ^{18}O changes. This conclusion, although being based on idealised simulations with no possible direct applications to proxy interpretation, highlights the caveats of relating local changes in δ^{18}O to local temperature changes, when neglecting the geographical context and hence the impact of changing atmospheric circulation patterns. Beyond this qualitative approach (which would require a detailed analysis of phenomena we briefly touched upon), the next section will concentrate on a quantitative case-study of the δ^{18}O-temperature relationship over Scandinavia.

4.4 Impact of seasonality on the δ^{18}O-temperature relationship over Scandinavia

The previous section highlights the need to jointly consider the geographical patterns of temperature and δ^{18}O changes (and hence the role of atmospheric circulation). Bearing this in mind, we now want to concentrate on the impact of changing seasonality on the δ^{18}O-temperature relationship over Scandinavia. The study region is comprised between 0°and 30°in longitude and 55°and 71°in latitude and encompasses 55 grid-

cells. The previous analysis revealed that the study region does not undergo severe changes related to oscillating planetary waves in the considered simulations.

Figure 5 presents the climatology (i.e. mean annual cycle) of precipitation, δ^{18}O and temperature over the study area. The temperature climatology (Fig. 5c) is very similar in all three simulations, with a maximum of 14°C in July–August and a minimum of −2°C in January–February. The δ^{18}O signal also shows a pronounced seasonal cycle, but the mid-Holocene simulation shows a 1‰ enrichment in summer compared with the other two runs (Fig. 5b). The precipitation climatology, which had not been addressed in the previous section, shows most distinct behaviours between the three simulations (Fig. 5a). While all simulations reproduce a maximum in autumn, the latter is more pronounced and earlier in the "present", a twofold peak for the "pre-industrial" and a later, weaker peak for the "mid-Holocene" simulation. This highlights a fundamental feature in climate change: as the external forcings vary, the atmospheric circulation and land-surface processes are affected, which can significantly modify both the amount and the timing of precipitation over a given area. This has severe consequences for the interpretation of the δ^{18}O signal.

The two lower subfigures in Fig. 5d–e show the linear regression for all grid-cell values over the 5-year experiment period (275 points in total). In the left (right) subfigure, mean (weighted) δ^{18}O in precipitation is plotted against annual mean (precipitation-weighted) temperature. The dashed lines indicate the confidence interval at 99% from the linear regression. For each plot, the regression coefficients are indicated below the plot. The regression uncertainty, preceded by +/− in the legend, expresses the mean of the confidence intervals over the regression domain (5% and 95% percentiles of the δ^{18}O values). The regression of mean annual temperature against mean weighted δ^{18}O is the conventional method (Fig. 5d). It does not account for the fact that, under the assumption that δ^{18}O is a suitable proxy for temperature, it only records it when precipitation occurs. This bias is corrected by weighing the monthly temperature with the monthly precipitation amount, consistently with the way annual (weighted) δ^{18}O is computed (Fig. 5e).

Several conclusions can be drawn from the regressions on Fig. 5. $\delta^{18}O$ is in first order a good indicator for temperature in regions not directly affected by circulation changes. The regression factor $\frac{\Delta T}{\Delta \delta^{18}O}$ is close to 1.8°C‰$^{-1}$ for all simulations. Hence a 3‰ drop in mean annual $\delta^{18}O$ between present and mid-Holocene would imply a temperature drop by 5.5°C. The difference in spatial slopes between the "present" (1.84°C‰$^{-1}$) and "mid-Holocene" (1.80°C‰$^{-1}$) spatial slopes implies an error of 0.12° C, which is smaller than the 99% confidence interval (0.5° C). When considering the regression of precipitation-weighted temperature, the spread is reduced as expressed by the 40% decrease in the 99% confidence interval: this indicates that the weighing better captures the physical relationships between temperature and $\delta^{18}O$. Since most of the precipitation occurs at a season warmer than the annual mean, the regression factor $\frac{\Delta T}{\Delta \delta^{18}O}$ is lower (1.5°C‰$^{-1}$ versus 1.8°C‰$^{-1}$). In this case, a 3‰ drop in $\delta^{18}O$ would imply a 4.5°C drop in weighted temperature. Yet the difference between the spatial slopes under present and mid-Holocene conditions imply an error in the order of 0.42°C, which is this time larger than the 99% confidence interval (0.3°C).

It is beyond the scope of the present article to discuss the validity of the regressions presented above. The regression coefficients rely on idealised experiments which likely underestimate the actual differences in temperature and $\delta^{18}O$ between present and mid-Holocene climate conditions. Furthermore, computing spatial regression slopes over a larger domain makes the implicit assumption that the isotopic signal is uniform over the area. This assumption, even though it might be valid from a statistical point of view in the considered simulation, is contradicted by higher resolution simulations. A study of the isotopic signature of the North Atlantic Oscillation (Sturm et al., 2009) shows distinct responses between Northern and Southern Scandinavia. Hence a confrontation of the simulations with observations and multiple proxy data would be needed before concluding on the validity of the paleo-thermometer over Scandinavia. On the other hand, the regression analysis presented above highlights the issue of seasonality when interpreting isotopic proxy data. An empirical regression based on present-day

CPD
5, 1697–1729, 2009

data might reconstruct (unknowingly) precipitation-weighted temperature, assuming it represents mean annual temperature. The comparison between the weighted and unweighted regression coefficients shows that this might introduce an overestimation of the temperature change by more than 20%.

5 Conclusions

The isotopic signal in climate archives is a strong climate proxy, yet difficult to interpret because it is influenced by a wide range of climate processes. The δ^{18}O signal is commonly interpreted as an indicator for temperature, which requires a calibration under present-day conditions. While δ^{18}O at mid- to high latitudes is generally well correlated with temperature, this relationship only holds as long as the dominant atmospheric patterns and the seasonal distribution of precipitation remains stable. Climate models with embedded stable water isotope diagnostics can be used as a tool to assess the robustness of the δ^{18}O-temperature relationship under different climate conditions, as well as to provide confidence (i.e. uncertainty) intervals for the climate reconstruction. The purpose of the present article is to support the use of isotope-enabled climate models for providing physically-based "transfer functions" between the isotopic signal and climate, in order to exploit most of the information enclosed in isotopic climate archives. A particular advantage compared to conventional paleo-climatological methods is the ability to make a spatial synthesis of multiple proxies, to give way to the assimilation of multiple isotopic proxy data. Further model developments are needed to make the proxy assimilation possible for terrestrial isotopic archives. At present, the forward proxy modelling is restricted to the isotopic composition of precipitation. With the exception of ice-cores, isotopic proxy records do not record directly the precipitation of δ^{18}O. Hence, local hydrological and biogeochemical processes need to be implemented in the model, so that the simulated "pseudo-proxy" can directly be compared with the measured isotopic signal in the climate archive. For instance, implementing the isotopic tracers in an hydrological model allows the representation of the isotopic

composition of lake-water, from which biological parametrisations can derive the $\delta^{18}O$ of e.g. algae cellulose and ostracode calcite in the model world (hence pseudo-proxy). This approach will account e.g. for the convolution of melt-water pulses, evaporative enrichment over the lake and the timing of the algae/ostracode growing season under various climate conditions. The pseudo-proxy record can then directly be compared with the observed (isotopic) proxy record. The same procedure can be applied to $\delta^{18}O$ in tree-rings and speleothem records, with the application of ad-hoc soil infiltration, tree physiology or cave models. The advantage of such a forward (pseudo-) proxy method is that the sensitivity of the climate reconstruction to phenomena (atmospheric circulation changes, seasonality) can be tested, which is out of reach for empirical regression methods. Finally, the sum of data provided by ensemble simulations and modelling sensitivity studies can provide a quantitative assessment of the uncertainties associated with climate reconstructions from combined proxy and modelling evidence.

Acknowledgements. This work is a result of the workshop on Holocene climate variability over Scandinavia, hosted by the Bert Bolin Centre for Climate Research, Stockholm University, in April 2008. The collaboration between Q. Zhang and D. Noone on CAM3iso modelling was made possible thanks to a visiting grant from the International Meteorological Institute.

References

Bariac, T., Gonzalez-Dunia, J., Katerji, N., Béthenod, O., Bertolini, J. M., and Mariotti, D.: Spatial variation of the isotopic composition of water (^{18}O, ^{2}H) in organs of aerophytic plants: 2. Assessment under field conditions, Chem. Geol., 115, 317–333, 1994. 1707

Berger, A. L.: Long-Term Variations of Daily Insolation and Quaternary Climatic Changes, J. Atmos. Sci., 35, 2362–2367, doi:10.1175/1520-0469(1978)035<2362:LTVODI>2.0.CO;2, 1978. 1712, 1725

Bjerknes, V.: The meteorology of the temperate zone and the general atmospheric circulation, Mon. Weather Rev., 49, 1–3, doi:10.1175/1520-0493(1921)49<1:TMOTTZ>2.0.CO;2, 1921. 1705

Dansgaard, W.: Stable isotopes in precipitation, Tellus, XVI, 436–468, 1964. 1700

EPICA: EPICA team: Augustin, L., Barbante, C., Barnes, P. R. F., Barnola, J. M., Bigler, M., Castellano, E., Cattani, O., Chappellaz, J., Dahl-Jensen, D., Delmonte, B., Dreyfus, G., Durand, G., Falourd, S., Fischer, H., Flückiger, J., Hansson, M. E., Huybrechts, P., Jugie, G., Johnsen, S. J., Jouzel, J., Kaufmann, P., Kipfstuhl, J., Lambert, F., Lipenkov, V. Y., Littot, G. C., Longinelli, A., Lorrain, R., Maggi, V., Masson-Delmotte, V., Miller, H., Mulvaney, R., Oerlemans, J., Oerter, H., Orombelli, G., Parrenin, F., Peel, D. A., Petit, J. R., Raynaud, D., Ritz, C., Ruth, U., Schwander, J., Siegenthaler, U., Souchez, R., Stauffer, B., Steffensen, J. P., Stenni, B., Stocker, T. F., Tabacco, I. E., Udisti, R., van de Wal, R. S. W., van den Broeke, M., Weiss, J., Wilhelms, F., Winther, J. G., Wolff, E. W., and Zucchelli, M., Eight glacial cycles from an Antarctic ice core, Nature, 429, 623–238, 2004. 1701

ECMWF (European Center for Mid-term Weather Forecast): ERA40 data centre, online available at: http://data-portal.ecmwf.int/data/d/era40_moda/, 2003. 1710

Gates, W. L., Boyle, J. S., Covey, C., Dease, C. G., Doutriaux, C. M., Drach, R. S., Fiorino, M., Gleckler, P. J., Hnilo, J. J., Marlais, S. M., Phillips, T. J., Potter, G. L., Santer, B. D., Sperber, K. R., Taylor, K. E., and Williams, D. N.: An Overview of the Results of the Atmospheric Model Intercomparison Project (AMIP I), B. Am. Meteorol. Soc., 80, 29–55, doi:10.1175/1520-0477(1999)080<0029:AOOTRO>2.0.CO;2, 1999. 1711

Hack, J., Hurrell, J., Rosinski, J., and Caron, J.: The NCAR CGD annual Scientific report 2002, Tech. rep., NCAR, 2002. 1712

Hoffmann, G., Werner, M., and Heimann, M.: Water isotope module of the ECHAM atmospheric general circulation model: A study on timescales from days to several years, J. Geophys. Res., 103, 16871–16896, 1998. 1699, 1723

Johnsen, S., Dahl-Jensen, D., Dansgaard, W., and Gundestrup, N.: Greenland paleotemperatures derived from GRIP bore hole temperature and ice core isotopic profiles, Tellus, 47B, 624–629, doi:10.1034/j.1600-0889.47.issue5.9.x, http://www.blackwell-synergy.com/doi/abs/10.1034/j.1600-0889.%47.issue5.9.x, 1995. 1701

Johnsen, S. J., Dahl-Jensen, D., Gundestrup, N., Steffensen, J. P., Clausen, H. B., Miller, H., Masson-Delmotte, V., ornsdottir, A. E. S., and White, J.: Oxygen isotope and palaeotemperature records from six Greenland ice-core stations: Camp Century, Dye-3, GRIP, GISP2, Renland and NorthGRIP, J. Quaternary Sci., 16, 299–307, 2001. 1702

Joussaume, J., Sadourny, R., and Jouzel, J.: A general circulation model of water isotope cycle in the atmosphere, Nature, 311, 24–29, 1984. 1707

Joussaume, S. and Taylor, K. E.: Status of the Paleoclimate Modeling Intercomparison Project,

in: Proceedings of the first international AMIP scientific conference, WCRP-92, Monterey, USA, 425–430, 1995. 1711

Jouzel, J. and Merlivat, L.: Deuterium and oxygen 18 in precipitation: modeling of the isotopic effects during snow formation, J. Geophys. Res., 89, 11749–11757, 1984. 1707

Jouzel, J., Lorius, C., Petit, J. R., Genthon, C., Barkov, N. I., Kotlyakov, V. M., and Petrov, V. M.: Vostok ice core: a continuous isotope temperature record over the last climatic cycle (160000 years), Nature, 329, 402–408, 1987a. 1701

Jouzel, J., Russel, G. L., Suozzo, R. J., Koster, R. D., White, J. W., and Broecker, W. S.: Simulations of the HDO and $H_2^{18}O$ atmospheric cycles using the NASA/GISS general circulation model: the seasonal cycle for present-day conditions, J. Geophys. Res., 92, 14739–14760, 1987b. 1699, 1707

Jouzel, J., Alley, R. B., Cuffey, K. M., Dansgaard, W., Grootes, P., Hoffmann, G., Jonsen, S. J., Koster, R. D., Peel, D., Shuman, C. A., Stievenard, M., Stuiver, M., and White, J. W.: Validity of the temperature reconstruction from water isotopes in ice cores, J. Geophys. Res., 102, 26471–26487, 1997. 1701

Kurita, N., Sugimoto, A., Fujii, Y., Fukazawa, T., Makarov, V. N., Watanabe, O., Ichiyanagi, K., Numaguti, A., and Yoshida, N.: Isotopic composition and origin of snow over Siberia, J. Geophys. Res., 110, D13102, doi:{10.1029/2004JD005053}, http://dx.doi.org/10.1029/2004JD005053, 2005. 1723

Lee, J.-E., Fung, I., DePaolo, D. J., and Henning, C. C.: Analysis of the global distribution of water isotopes using the NCAR atmospheric general circulation model, J. Geophys. Res., 112, D16306, doi:10.1029/2006JD007657, http://www.agu.org/pubs/crossref/2007/2006JD007657.shtml, 2007. 1723

Majoube, M.: Fractionnement en oxygène 18 et en deutérium entre l'eau et sa vapeur, J. Chem. Phy., 10, 1423–1436, 1971. 1706

Mathieu, R., Pollard, D., Cole, J. E., White, J. W. C., Webb, R. S., and Thompson, S. L.: Simulation of stable water isotope variations by the GENESIS GCM for modern conditions, J. Geophys. Res., 107(D4), 4037, doi:10.1029/2001JD900255, 2002. 1723

Merlivat, L. and Jouzel, J.: Global climatic interpretation of the deuterium-oxygen 18 relationship for precipitation, J. Geophys. Res., 84, 5029–5033, 1979. 1707

Rapley, C. and Grassl, H.: The GNIP Booklet, online available at: http://www-naweb.iaea.org/napc/ih/GNIP/userupdate/description/1stpage.html, last access: June 2009. 1700, 1708

Schmidt, G. A., LeGrande, A. N., and Hoffmann, G.: Water isotope expressions of intrinsic and

forced variability in a coupled ocean-atmosphere model, J. Geophys. Res., 112, D10103, doi:10.1029/2006JD007781, http://www.agu.org/pubs/crossref/2007/2006JD007781.shtml, 2007. 1723

Solomon, S., Qin, D., Manning, M., Alley, R., Berntsen, T., Bindoff, N., Chen, Z., Chidthaisong, A., Gregory, J., Hegerl, G., Heimann, M., Hewitson, B., Hoskins, B., Joos, F., Jouzel, J., Kattsov, V., Lohmann, U., Matsuno, T., Molina, M., Nicholls, N., Overpeck, J., Raga, G., Ramaswamy, V., Ren, J., Rusticucci, M., Somerville, R., Stocker, T., Whetton, P., Wood, R., and Wratt, D.: Climate Change 2007: The Physical Science Basis. Contribution of Working Group I to the Fourth Assessment Report of the Intergovernmental Panel on Climate Change, Cambridge University Press, http://ipcc-wg1.ucar.edu/wg1/wg1-report.html, 2007. 1698

Sturm, C. K., Hoffmann, G., Langmann, B., and Stichler, W.: Simulation of $\delta^{18}O$ in precipitation by the regional circulation model $REMO_{iso}$, Hydrol. Process., 19, 3425–3444, doi:10.1002/hyp.5979, 2005. 1708

Thompson, L. G.: Ice core evidence for climate change in the Tropics: implications for our future, Quaternary Sci. Rev., 19, 19–35, doi:10.1016/S0277-3791(99)00052-9, http://www.sciencedirect.com/science/article/B6VBC-40378TB-4/2/1f08f9aa12b72d0097d8d4cfd526f30a, 2000. 1702

Vimeux, F., Gallaire, R., Bony, S., Hoffmann, G., and Chiang, J. C.: What are the controls on δD in precipitation in the Zongo Valley (Bolivia) ? Implications for the Illimani ice core interpretation, Earth Planet. Sci. Lett., 240(2), 205–220, ISSN 0012-821X, doi:10.1016/j.epsl.2005.09.031, 2005. 1702

Werner, M., Mikolajewicz, U., Heimann, M., and Hoffmann, G.: Borehole versus isotope temperatures on Greenland: seasonality does matter, Geophys. Res. Lett., 27, 723–726, 2000. 1702

Yoshimura, K., Kanamitsu, M., Noone, D., and Oki, T.: Historical isotope simulation using Reanalysis atmospheric data, J. Geophys. Res.h, 113, D19108, doi:{10.1029/2008JD010074}, http://www.agu.org/pubs/crossref/2008/2008JD010074.shtml, 2008. 1723

Table 1. Stable water isotope enabled GCM, participating in the 2nd Stable Water Isotope iNtercomparison Group (SWING2). W.i.p indicates work in progress. More information on the SWING2 project can be found on http://people.su.se/~cstur/SWING2/.

Model	Institute	References
CAM3	U. Colorado	Noone et al., w.i.p.
CAM2	UC Berkeley	Lee et al. (2007)
ECHAM5	AWI-Bremerhaven	Werner et al., w.i.p.
ECHAM4	MPI-Hamburg	Hoffmann et al. (1998)
LMDZ4	LMD-Paris	Risi et al., submitted
MIROC3.2	JAMSTEC-Yokosuka	Kurita et al. (2005)
GSM	Scripps-San Diego	Yoshimura et al. (2008)
GISS-E	GISS-New York	Schmidt et al. (2007)
GENESIS	Penn U.	Mathieu et al. (2002)
ACCESS	ANSTO-Sydney	Fischer et al., w.i.p.
HadCM3	U. Bristol	Tindall et al., w.i.p.
HadAM3	BAS	Sime et al., w.i.p.

Table 2. Greenhouse gases and Earth's orbital parameters in three simulations.

	Present	Pre-industrial	mid-Holocene
CO_2 (ppmv)	348	280	280
CH_4 (ppbv)	1650	760	650
NO_2 (ppbv)	306	270	270
Eccentricity	0.0167724	0.0167724	0.018682
Obliquity (°)	23.446	23.446	24.105
Angular precession	102.04	102.04	0.87

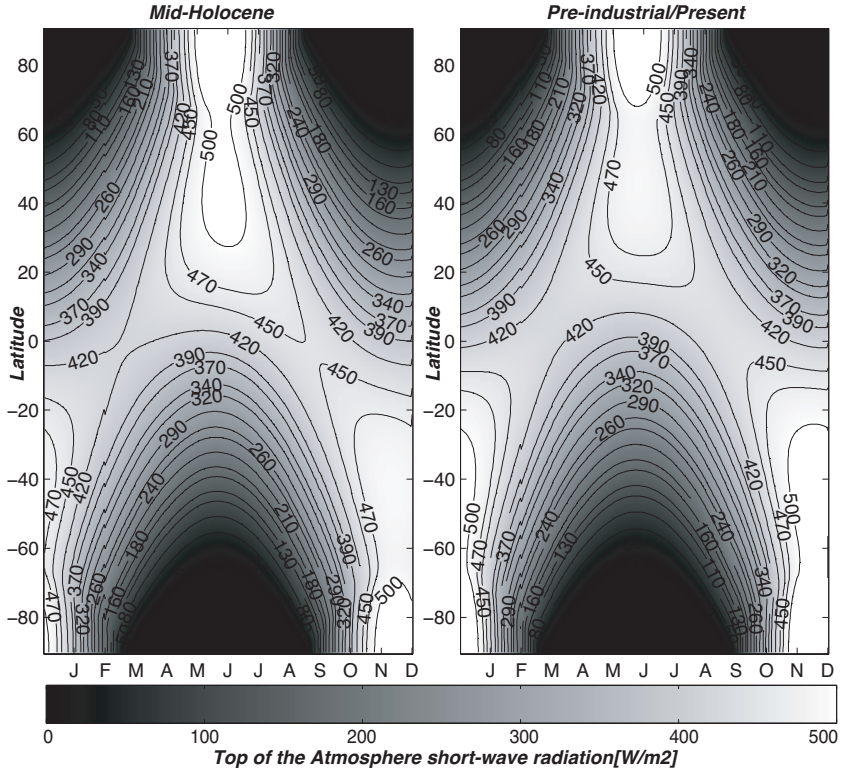

Fig. 1. Comparison of the top-of-the-atmosphere shortwave radiation (i.e. insolation), between the mid-Holocene (left) and present (right) situation. The vertical axis represents the latitudes (as the insolation is constant over a given longitude), the horizontal axis represents the month of the year. The seasonal distribution and total intensity of the solar radiation is computed according to the orbital parameters indicated in Table 2 (Berger, 1978).

CPD
5, 1697–1729, 2009

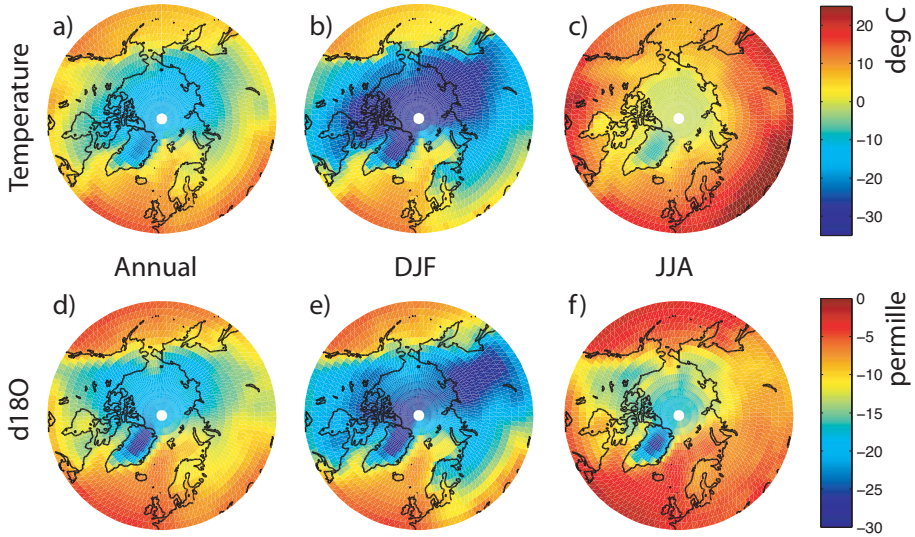

Fig. 2. Stereographic plots of the Northern Hemisphere (at latitudes above 45 degrees) for the reference (pre-industrial) simulation. In the upper (lower) row, the temperature (δ^{18}O in precipitation) is shown. The left column displays the annual mean, the middle column the winter (DJF) mean and the right column the summer (JJA) mean. The colour bars are common to all subfigures in the row.

CPD
5, 1697–1729, 2009

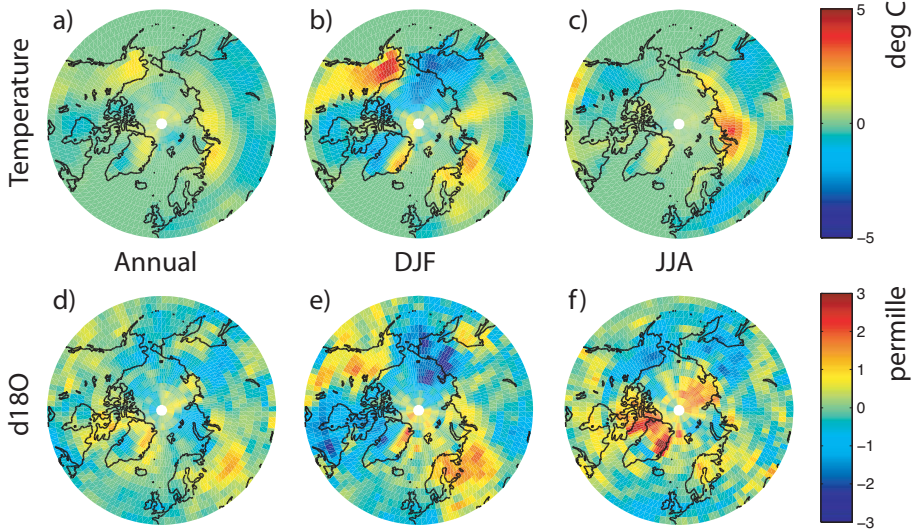

Fig. 3. Using the same projection as in Fig. 2, the difference between the present and the reference (pre-industrial) simulations for temperature (upper row) and δ^{18}O (lower row), for annual (left column), winter (central column) and summer (right column) means.

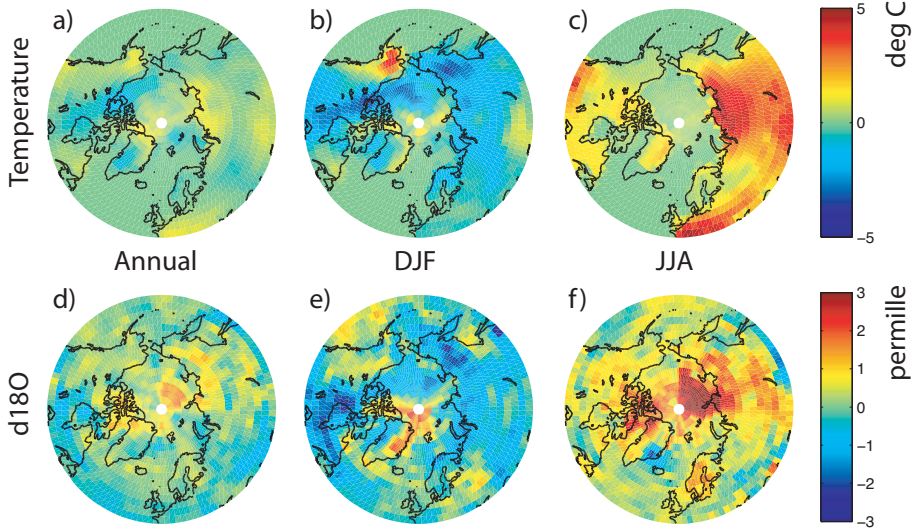

Fig. 4. The sub-figures are identical to Fig. 3 for the differences between Mid-Holocene and the reference simulation.

CPD
5, 1697–1729, 2009

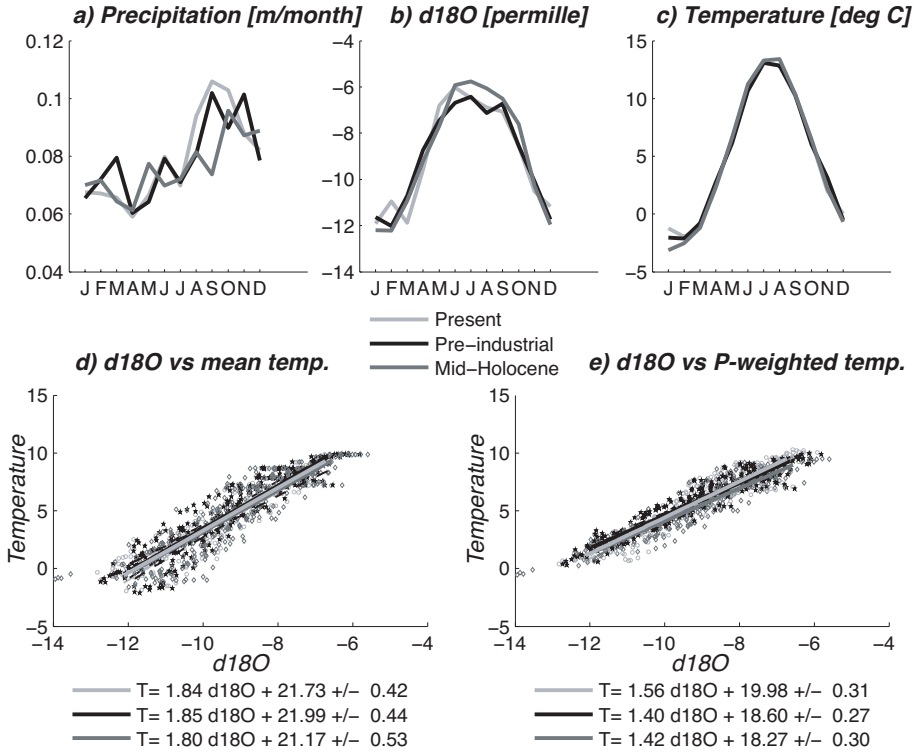

Fig. 5. The figure presents the impact of seasonality on the δ^{18}O signal. The upper row shows the climatology of precipitation (left), δ^{18}O in precipitation (middle) and temperature (right) averaged over Scandinavia. The lower row shows the linear regression of mean temperature against δ^{18}O with the corresponding regression equation (and mean confidence intervals) shown below the graph. The left (right) graph shows the regression of mean annual (precipitation-weighted) temperature against δ^{18}O.

CPD
5, 1697–1729, 2009